

# Electronically Excited States in Poly(*p*-phenylenevinylene): Vertical Excitations and Torsional Potentials from High-Level Ab Initio Calculations

Aditya N. Panda,<sup>†,‡</sup> Felix Plasser,<sup>§</sup> Adelia J. A. Aquino,<sup>||,⊥</sup> Irene Burghardt,<sup>\*,‡,#</sup> and Hans Lischka<sup>\*,§,⊥</sup>

<sup>†</sup>Department of Chemistry, Indian Institute of Technology Guwahati, Guwahati, 781039, Assam, India

<sup>‡</sup>Département de Chimie, Ecole Normale Supérieure, 24 rue Lhomond, 75231 Paris Cedex 05, France

<sup>§</sup>Institute of Theoretical Chemistry, University of Vienna, Währingerstrasse 17, A-1090, Vienna, Austria

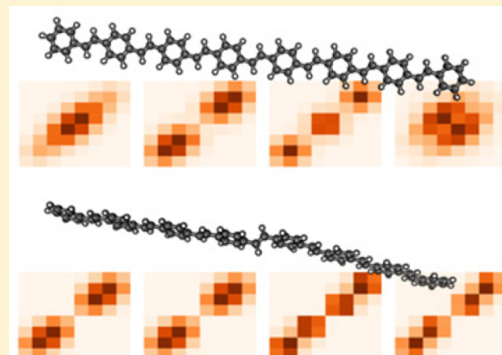
<sup>||</sup>Institute of Soil Research, University of Natural Resources and Life Sciences, Peter-Jordan-Strasse 82, A-1190, Vienna, Austria

<sup>⊥</sup>Department of Chemistry and Biochemistry, Texas Tech University, Lubbock, Texas 79409-1061, United States

<sup>#</sup>Institute of Physical and Theoretical Chemistry, Goethe University, Max-von-Laue-Strasse 7, 60438 Frankfurt am Main, Germany

## Supporting Information

**ABSTRACT:** Ab initio second-order algebraic diagrammatic construction (ADC(2)) calculations using the resolution of the identity (RI) method have been performed on poly-(*p*-phenylenevinylene) (PPV) oligomers with chain lengths up to eight phenyl rings. Vertical excitation energies for the four lowest  $\pi-\pi^*$  excitations and geometry relaxation effects for the lowest excited state ( $S_1$ ) are reported. Extrapolation to infinite chain length shows good agreement with analogous data derived from experiment. Analysis of the bond length alternation (BLA) based on the optimized  $S_1$  geometry provides conclusive evidence for the localization of the defect in the center of the oligomer chain. Torsional potentials have been computed for the four excited states investigated and the transition densities divided into fragment contributions have been used to identify excitonic interactions. The present investigation provides benchmark results, which can be used (i) as reference for lower level methods and (ii) give the possibility to parametrize an effective Frenkel exciton Hamiltonian for quantum dynamical simulations of ultrafast exciton transfer dynamics in PPV type systems.



## 1. INTRODUCTION

Poly-(*p*-phenylenevinylene) (PPV, Scheme 1a) plays a paradigmatic role in understanding the electronically excited states and the excitation energy transfer (EET) in conjugated organic molecules to be used in electronic devices aiming at applications in photovoltaics and electroluminescence.<sup>1–5</sup> Understanding the EET at a molecular level is of fundamental importance for a successful design of efficient photovoltaic devices. Recent experiments have shown fascinating features of coherent PPV dynamics<sup>5</sup> and a rationalization in terms of structural dynamics along the PPV chain has been suggested.<sup>6</sup> It is well documented that a structural relaxation in connection with the evolution of the electronically excited states plays an important role for the EET dynamics.<sup>7</sup> These processes are coupled in a complex way because at least several electronic states are involved and nonadiabatic effects have to be considered due to crossings of these states depending on their structural evolution.

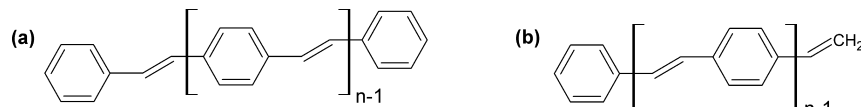
Electronic structure calculations have the potential to clarify the above-addressed questions but are facing severe problems because of the large molecular sizes to be handled in addition to the already extremely difficult task of calculating reliably the

required electronic states. In view of this situation, several semiempirical calculations have been performed using the collective electronic oscillator (CEO) method combined with the Austin Model 1 (AM1)<sup>8</sup> applied to PPV and to polyphenylene ethynylene units<sup>9</sup> and the Pariser–Parr–Pople (PPP)  $\pi$  electron Hamiltonian<sup>10</sup> for surface hopping dynamics. The vibronic structure of the lowest optical transitions in PPV has been studied using a monoexcited configuration interaction for the electronic transition and an empirical description of the electron phonon coupling.<sup>11</sup> The torsional dependence of the potential energy surface for the first excited state around the vinylene single bonds was investigated by means of Zerner's intermediate neglect of differential overlap (ZINDO) method<sup>12</sup> and comparison was made with time-dependent density functional theory (TDDFT) results. The TDDFT method has been used also to study the singlet–triplet splitting in oligomers of  $\alpha$ -thiophenes, *p*-phenylenes, PPV, and ladder-type oligophenylenes.<sup>13</sup> Furthermore, the localization of the

**Received:** January 11, 2013

**Revised:** February 18, 2013

**Published:** February 21, 2013

**Scheme 1.** Structures of (a)  $(PV)_n P$  and (b)  $(PV)_n$ 

electronic excitation along the polymeric PPV chains in dependence of different functionals was investigated.<sup>14</sup> In a subsequent publication by the same authors<sup>15</sup> environmental polarization has been included noting that the localization of charged polarons was sensitive to environmental polarization whereas neutral states were less affected. Following a different approach, a diabatic Hamiltonian for application to wavepacket dynamics in PPV driven by torsional modes along the vinylene single bonds and the bond length alternation has been developed.<sup>16</sup> Intrachain vs interchain energy transfer dynamics has been studied in conjugated polymers on the basis of Förster-type approaches<sup>17</sup> and interactions between linked chromophoric units in MEH-PPV have been modeled by the kinetic Monte Carlo method<sup>18</sup> to compute the fluorescence depolarization in poly-[2-methoxy-5-((2-ethylhexyl)oxy)-phenylenevinylene] (MEH-PPV).

Ab initio investigations are much more costly than semiempirical or TDDFT calculations and, therefore, the focus concentrated on the smaller oligomers of PPV starting with complete active space perturbation theory to second-order (CASPT2) calculations on the electronic spectrum of stilbene<sup>19</sup> to symmetry-adapted cluster-configuration interaction (SAC-CI) investigations up to four PV units.<sup>20</sup> Torsional motions around the vinylene single and double bonds and the location of conical intersections have been investigated at complete active space self-consistent field (CASSCF) and CASPT level for stilbene.<sup>21</sup> Whereas these methods have been shown to provide reliable data for electronically excited states of  $\pi$ -conjugated oligomers, their scope in terms of oligomer sizes is quite limited because of the drastically growing computational cost with increasing chain length. To satisfy the urgent demand for ab initio investigations for significantly larger oligomer length, the approximate coupled cluster method to second-order (CC2)<sup>22</sup> has been shown to be very useful in calculations on methylene-bridges oligofluorenes<sup>23</sup> and oligo-*p*-phenylenes.<sup>24</sup> The combination with the resolution of the identity (RI) method<sup>25</sup> allowed computationally efficient calculations on several excited states and the availability of analytic energy gradients for excited states<sup>26</sup> proved to be an especially interesting feature. A systematic benchmark investigation on the capabilities of the CC2 method can be found in ref 27. The related second-order algebraic construction method (ADC(2)) method<sup>28,29</sup> gives similar results in comparison to CC2;<sup>29,30</sup> it has, however, the advantage over CC2 that the excited states are obtained as eigenvalues of a hermitian matrix whereas in coupled-cluster response the excitation energies are obtained as eigenvalues of a non-Hermitian Jacobi matrix.<sup>29</sup> It is, however, to be expected that the second-order character of the method can lead to artifacts. Recent benchmark equation of motion excitation energy coupled-cluster (EOMEE-CC) calculations on DNA nucleobases<sup>31</sup> and comparison with CC2 led to the conclusion that CC2 reproduced  $\pi-\pi^*$  excitations remarkably well in comparison to the higher-level EOMEE-CC approach with singles and doubles and noniterative triples (CCSD(T)) method. CC2 showed noteworthy deficiencies primarily in describing  $n-\pi^*$  states, a type of excitation not relevant for the

UV spectrum of PPV. Because of the aforementioned similarity of ADC(2) to CC2 it can be expected that the former method will show similar good performance for  $\pi-\pi^*$  states.

One major goal of this work is to provide reliable and consistent information on the excited state properties of PPV oligomers such as vertical excitation energies, torsional potentials, and defect localization in the  $S_1$  state for extended oligomer sizes using the aforementioned RI-ADC(2) method. Even though the TDDFT method would be clearly preferred because of its computational efficiency, we decided for the ADC(2) method because it is free of any ambiguities of choosing an appropriate density functional. Such choices between different functionals will be critical because it has been shown that the defect localization (self-trapping of the exciton) strongly depends on the amount of Hartree–Fock exchange included in the selected functional.<sup>14</sup> PPV consists of alternating phenylene and vinylene units, which are connected through  $\pi$ -conjugation. The structure of the excited states is determined by the interplay between states deriving from phenylene and vinylene units as well as by defects in the molecular structure. The nature of the excited states in PPV is still a matter of debate. Thus, our second goal is to get more insight into the electronic mechanism of interaction between different subunits and to characterize the electronic nature of the excitons using previously developed methods based on the analysis of transition density matrices.<sup>32</sup> For that purpose two types of oligomers representing PPV have been chosen: (i) the phenyl end-capped version denoted  $(PV)_n P$  and (ii) the vinylene end-capped oligomer denoted  $(PV)_n$ . Here P and V denote phenyl and vinyl units, respectively. The purpose of these two choices was to investigate the effect of the different chain terminations on geometry and UV spectra. Aside from the electronic nature of the excitons, geometric distortions are important. The phenomenon of exciton–phonon coupling and its relation to exciton localization has been studied by several groups.<sup>10,33–35</sup> Moreover, it has been pointed out that defects breaking the electronic coupling are of highest interest.<sup>5,36,37</sup> Torsional coordinates around the junctions between the vinylene and phenylene subunits have been studied in this work as they play a prominent role as has been shown in simulations of the vibrational broadening of the UV spectrum<sup>12</sup> and in the photodynamics following the absorption process.<sup>10,38</sup> Additionally, we have investigated the bond length alternation (BLA)<sup>10</sup> computed from bond length differences for the interring junction and within the phenylene units relevant for the trapping of defects. Finally, this work is also aiming at the preparation of the basis to fit parameters to our ab initio data to be used in diabatic Hamiltonians<sup>16,39</sup> and subsequent wavepacket dynamics simulations.

## 2. COMPUTATIONAL DETAILS

All excited state calculations were performed at the ADC(2) level.<sup>28,29</sup> Ground state geometry optimizations were carried out using the Møller–Plesset perturbation theory to second-order (MP2).<sup>40</sup> In both cases the RI approximation<sup>29,41–43</sup> and the SV(P)<sup>44</sup> basis was used. All vertical excitations were

computed using the SV(P) and TZVP<sup>45</sup> basis sets; for the smaller oligomers the TZVPP basis<sup>41</sup> was used as well. For (PV)<sub>7</sub>P and (PV)<sub>8</sub> torsional potential curves and the geometry optimization in the S<sub>1</sub> state were performed with the split valence SV basis for reasons of computational economy by removing the polarization functions from the SV(P) basis set.

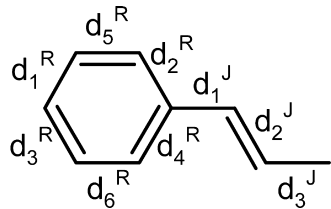
For a compact characterization of the molecular structure the following two BLA parameter definitions were used following ref 10

$$d^R = 0.25(d_1^R + d_2^R + d_3^R + d_4^R) - 0.5(d_5^R + d_6^R) \quad (1)$$

$$d^J = 0.5(d_1^J + d_3^J) - d_2^J \quad (2)$$

Here the  $d_i^R$  refer to bond distances within a ring R whereas the  $d_i^J$  refer to bond lengths in the vinyl junction J. The labeling of the bonds within one unit is shown in Scheme 2.

**Scheme 2. Bond Labeling Scheme Used for One PV Unit**



The symmetry of the planar (PV)<sub>n</sub>P structures is C<sub>2h</sub> and that of (PV)<sub>n</sub> is C<sub>s</sub>. Rigid torsional potential curves (i.e., in the absence of geometry optimization for the remaining coordinates) in C<sub>2</sub> symmetry were computed for (PV)<sub>n</sub>P by considering the four torsions labeled T<sub>1</sub>, T<sub>2</sub>, T<sub>3</sub>, and T<sub>4</sub> (Scheme 3) individually. The torsions were defined as linear combinations of individual torsional angles  $\tau$  as given, e.g., for T<sub>1</sub> as  $\tau_{23,24,25} + \tau_{23,24,25'}$ . The indices characterizing the angles refer to the bond numbers shown in Scheme 3. For simplicity, only  $\tau_{23,24,25}$  is given in the flowing text to characterize T<sub>1</sub>. Analogous definitions were adopted for the torsions T<sub>2</sub> to T<sub>4</sub>. To preserve C<sub>2</sub> symmetry, the symmetry equivalent bond on the other side of the molecule was twisted as well. The same definitions (without C<sub>2</sub> symmetry equivalence) were used also for (PV)<sub>8</sub>.

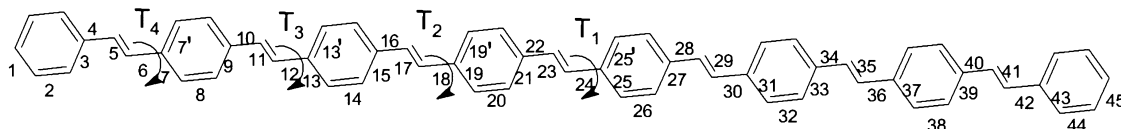
An extrapolation of the S<sub>1</sub> excitation energy to infinite chain lengths was performed according to the formula

$$E(N) = E_0 \sqrt{1 - 2\alpha \cos \frac{\pi}{N+1}} \quad (3)$$

suggested by Kuhn considering a linear chain of coupled oscillators<sup>46</sup> (see also ref 47 for a review). Here N refers to the number of linearly conjugated double bonds (two per phenylene and one per vinylene unit), i.e.

$$N = 3n + 2 \quad (4)$$

**Scheme 3. Structure and Numbering System of (PV)<sub>n</sub>P<sup>a</sup>**



<sup>a</sup>The four different torsional angles investigated are indicated as T<sub>1</sub>, T<sub>2</sub>, T<sub>3</sub>, and T<sub>4</sub>.

with n defined in Scheme 1. E(N) is the excitation energy at this chain length. The two parameters  $E_0$  and  $\alpha$  represent the excitation energy of an isolated oscillator and the coupling strength between neighboring oscillators, respectively. After taking the square of eq 3, the resulting formula

$$E(N)^2 = E_0^2 - E_0^2 2\alpha \cos \frac{\pi}{N+1} \quad (5)$$

may be readily used for a linear regression analysis against  $\cos(\pi/(N+1))$ .

The excited states were analyzed according to a recently developed scheme<sup>32</sup> based on previous work by Tretiak and Mukamel<sup>48</sup> and Luzanov and Zhikol.<sup>49</sup> For that purpose the transition density matrix  $D^{0\alpha[AO]}$  between the ground state and excited state  $\alpha$  expressed in the atomic orbital (AO) basis is considered. Furthermore, the system is partitioned into fragments A, B, ... Then the charge transfer number from fragment A to B for the transition to state  $\alpha$

$$\Omega_{AB}^\alpha = \frac{1}{2} \sum_{\substack{a \in A \\ b \in B}} (D^{0\alpha[AO]} S^{[AO]})_{ab} (S^{[AO]} D^{0\alpha[AO]})_{ab} \quad (6)$$

is computed by summation over basis functions a and b located on the respective fragments A, B, ... where the overlap matrix  $S^{[AO]}$  is used to account for nonorthogonality of the AOs in the sense of a Mulliken population analysis. For more details see ref 32. The charge transfer numbers take a more concrete meaning when the excited state is viewed as an *electron-hole* pair with respect to the ground state. Then  $\Omega_{AB}^\alpha$  can be understood as the probability of simultaneously finding the *hole* on fragment A and the *electron* on fragment B.

In the present study the analysis was carried out on the basis of PV fragments, where the formal cuts were performed through the vinyl double bonds. This choice was taken to have analogous fragments representing the overall symmetry of the molecule. Following ref 32 the ADC(2) singly excited cluster amplitudes were chosen to represent the transition density matrix because they dominate the expansion of the ADC(2) wave function.

### 3. RESULTS AND DISCUSSION

**3.1. Vertical Excitations.** The molecular structure of the (PV)<sub>n</sub>P ( $n = 1-7$ ) oligomers is presented in Scheme 1a. The planar ground state structures were optimized at the MP2/SV(P) level using C<sub>2h</sub> symmetry followed by the calculation of the four lowest vertical singlet excitation energies (1<sup>1</sup>B<sub>u</sub>, 2<sup>1</sup>A<sub>g</sub>, 2<sup>1</sup>B<sub>w</sub>, 3<sup>1</sup>A<sub>g</sub>). The excitation energies for the oligomer series computed at ADC(2)/TZVP level are plotted in Figure 1a as a function of the inverse number of double bonds N (eq 4). In the range from  $n = 4$  to  $n = 7$  an almost linear decrease between  $\Delta E$  and  $1/N$  is found for all states. The S<sub>1</sub> (1<sup>1</sup>B<sub>u</sub>) energy was fitted and extrapolated according to eq 5 using the data for (PV)<sub>n</sub>P ( $n = 2, \dots, 7$ ) with parameters  $E_0 = 9.775$  eV and  $\alpha = 0.456$ . This fit works remarkably well with a squared correlation

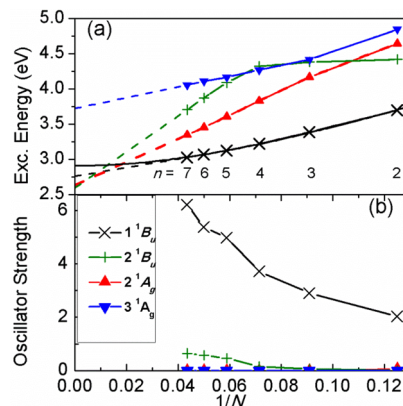


**Figure 1.** Vertical excitation energies (a) and oscillator strengths (b), computed at the ADC(2)/SV(P) level, for the first four excited states of different  $(PV)_n P$  oligomers plotted as a function of the inverse of chain length  $N$ . Extrapolations to  $N = \infty$  are shown as full line (Kuhn fit eq 3); dashed lines are the linear fits.

coefficient of 99.97% and a root mean squared error of only 0.004 eV. Extrapolation to  $N \rightarrow \infty$  yields a value of 2.91 eV for the polymer. A linear fit with the function  $A + B/N$  (Figure 1a) shows that the three lowest excited states  $S_1-S_3$ , lead to practically the same asymptotic values for  $N \rightarrow \infty$ , which suggests that these states derive from the same exciton band. In contrast, the fourth state ( $3^1A_g$ ) stays distinct at higher energies even at longer chain lengths with a polymer limit of 3.72 eV. Comparison of the fit linear in  $1/N$  with the Kuhn fit (eq 5) for the  $S_1$  state shows the well-known underestimation of the asymptotic limit by the former approach.<sup>47</sup> For the first members  $n = 2$  to  $n = 4$  in the  $(PV)_n P$  series the energy curve for the  $2^1B_u$  state is almost horizontal and starts with a linear decrease only for  $n \geq 5$ .

The oscillator strengths are plotted in Figure 1b. This figure shows that the lowest excited state ( $1^1B_u$ ) carries almost all the oscillator strength and that there is a strong increase with growing chain length. This increase in the oscillator strength is linear at the beginning of the series ( $n = 3-5$ ) and continues with a significantly enhanced rise for larger  $n$ . For longer

oligomers (starting with  $n = 5$ ) also the  $2^1B_u$  state possesses a nonnegligible, but still comparatively small, oscillator strength. The  $A_g$  states are dark for symmetry reasons. The direction of the transition dipole moments is shown in Figure 1S of the Supporting Information. They are in parallel to the molecular plane, pointing along the long molecular axis.

To explore the basis set effect of the vertical excitation energies in more detail, calculations using larger basis sets have been performed. The results are collected in Table 1. For  $n \leq 4$ , SV, SV(P), TZVP, and TZVPP basis sets have been used whereas for the larger oligomers ( $n = 5, 6$ , and  $7$ ) calculations have been carried out only with the SV, SV(P), and TZVP basis sets. Increasing the size of the basis set quite generally decreases the vertical excitation energies of all four excited states in relation to the ground state. The energy decreases by about 0.3 eV for all oligomers and all four states computed when going from SV to TZVP. It should be noted at this point that the SV basis does not contain any d-functions on C and that the SV(P) and SVP sets include one d-set on C. Extension to TZVPP (inclusion of an additional d-set and on one f-function) decreases the excitation energies further by about 0.1 eV for the  $n = 1, 2, 3$ , and  $4$  cases computed. Even though the basis set dependence of vertical excitation energies with respect to the ground state amounts to about 0.4–0.5 eV, it is also noted that the difference in the energies between the excited states remains almost constant within ~0.1 eV for all basis sets investigated (e.g., see the results for  $n = 7$  in Table 1). This is an important finding justifying the use of the relatively small SV basis for comparing the different excited states.

The computed vertical excitation energies show quite good agreement with the experimental results available for  $n = 1$  to  $n = 4$ .<sup>50</sup> Except for  $n = 1$  the TZVPP results are lower than the experimental values by 0.1–0.25 eV. The increase of the basis set will certainly increase the difference somewhat more. The value for the gasphase vertical excitation obtained from extrapolation of experimental oligomer spectra in solution is 3.25 eV (as computed from ref 47, Table 1, as  $\Delta E_{\text{vert}} = E_{00} + \Delta E_{\text{eq}}(\text{abs}) - \Delta E_{\text{solv}}$ ). Our value extrapolated to infinite chain length using the TZVP basis is 2.91 eV. The increase of the basis set to TZVPP for  $n = 1-4$  reduced the vertical excitation

**Table 1.** Basis Sets Effect on Vertical Excitation Energies (eV) Calculated at the ADC(2) Level Using Ground State Optimized Geometries of  $(PV)_n P$ ,  $n = 1-7^a$

		SV	SV(P)	TZVP	TZVPP		SV	SV(P)	TZVP	
$n = 1$	$1^1B_u$	4.781	4.542	4.394	4.274 (4.19)	$n = 5$	$1^1B_u$	3.455	3.216	3.126
	$2^1A_g$	4.958	4.844	4.737	4.688		$2^1A_g$	3.960	3.717	3.606
	$2^1B_u$	4.998	4.854	4.746	4.689		$2^1B_u$	4.457	4.229	4.088
	$3^1A_g$	6.377	6.105	5.936	5.791		$3^1A_g$	4.505	4.287	4.165
$n = 2$	$1^1B_u$	4.059	3.812	3.698	3.573 (3.69)	$n = 6$	$1^1B_u$	3.392	3.154	3.067
	$2^1B_u$	4.658	4.525	4.417	4.351		$2^1A_g$	3.798	3.557	3.453
	$2^1A_g$	4.904	4.779	4.645	4.571		$2^1B_u$	4.236	3.995	3.869
	$3^1A_g$	5.229	4.965	4.842	4.726		$3^1A_g$	4.443	4.225	4.105
$n = 3$	$1^1B_u$	3.728	3.486	3.385	3.258 (3.47)	$n = 7$	$1^1B_u$	3.351	3.113	3.027
	$2^1A_g$	4.527	4.309	4.165	4.048		$2^1A_g$	3.685	3.445	3.345
	$2^1B_u$	4.628	4.495	4.379	4.311		$2^1B_u$	4.062	3.820	3.703
	$3^1A_g$	4.687	4.516	4.414	4.320		$3^1A_g$	4.425	4.194	4.054
$n = 4$	$1^1B_u$	3.554	3.314	3.220	3.092 (3.34)					
	$2^1A_g$	4.196	3.953	3.829	3.706					
	$3^1A_g$	4.606	4.394	4.268	4.138					
	$2^1B_u$	4.592	4.454	4.320	4.231					

<sup>a</sup>Experimental values<sup>50</sup> are given in parentheses.

energy by another 0.1 eV and additional, smaller basis set effects could reduce the vertical excitation energy further, giving in summary an estimated value of 2.6–2.7 eV at ADC(2) level in the complete basis set limit. The discrepancies to the experimental value of 3.25 eV can be partly ascribed to inadequacies present in the ADC(2) approach, but possibly also to the reduction of the conjugation length in the PPV polymer due to kinks in the chains resulting from the flat  $S_0$  potential (see below) around the planar structures and a corresponding increase in the observed excitation energy.

**3.2. Geometry Relaxation in Ground and Excited States.** To characterize the geometries optimized for  $S_0$  and  $S_1$ , the BLA parameters as defined in eqs 1 and 2 were used. The results for the junctions and rings are shown in Figure 2a,b,

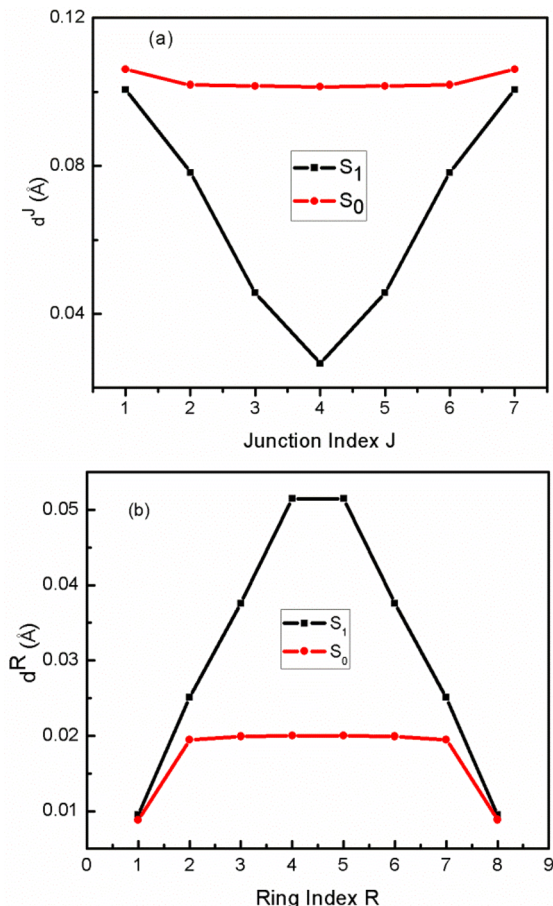


**Figure 2.** BLA values for (a) the vinylene junctions  $J$  and (b) for the phenylene rings  $R$  of  $(PV)_7P$ . The results are shown for the optimized geometries of the ground ( $S_0$ ) and first excited ( $S_1$ ) states using the ADC(2)/SV approach.

respectively, and the underlying bond distances are displayed in Figure 2S (Supporting Information). In the ground state (Figure 2a), all the vinylene junctions show a significant bond length alternation (e.g.,  $d^J \sim 0.10 \text{ \AA}$ ), indicating the pronounced difference between the single and double bonds. In the excited state  $d^J$  decreases significantly toward the center of the chain with a minimal value for  $d^J \approx 0.025 \text{ \AA}$ . The  $d^R$  BLA values for the phenylene units (Figure 2b) show a different trend. In the ground state the bond length alternation is very small ( $0.02 \text{ \AA}$ ), representing undistorted phenyl rings. In the  $S_1$  state a pronounced quinoid distortion, shortening of the bonds

5 and 6 and an increasing the bonds 1–4 in the phenylene units, is found. Again, this distortion is pronounced at the center, which can be understood as a trapping of the exciton. A similar picture of defect localization in the  $S_1$  state was given by Sterpone and Rossky<sup>10</sup> on the basis of combined PPP/force field calculations. The TDDFT study of Nayyar et al.<sup>14</sup> reflects the strong dependence of the defect localization on the density functional used. The general gradient approximation (GGA) functional PBE does not result in any significant defect confinement; increasing the amount of Hartree–Fock exchange leads to enhanced localization. The present ADC(2) results confirm the strongly localized picture with an extension of the trapping over about four repeat units.

The minimum to minimum  $S_0/S_1$  transition is 3.246 eV, as compared to the vertical excitation energy of 3.445 eV (Table 1, SV(P) basis). The resulting reduction of 0.199 eV is somewhat smaller than the experimental estimate  $\Delta E_{\text{eq}}$  of 0.28 eV.<sup>47</sup>

**3.3. Torsional Potentials.** Besides the BLA, the torsional interring modes around the vinylene single bonds are being considered as most important for the excitonic coupling of different PPV units.<sup>16</sup> Rigid torsional potential curves have been computed for the ground and the first four excited states of  $(PV)_7P$  along the four torsional angles,  $T_1$ ,  $T_2$ ,  $T_3$  and  $T_4$  (Scheme 3). The results were obtained by varying the torsional angles between the adjacent rings in  $30^\circ$  steps. Ground state torsions are shown in Figure 3. All four torsional curves are very

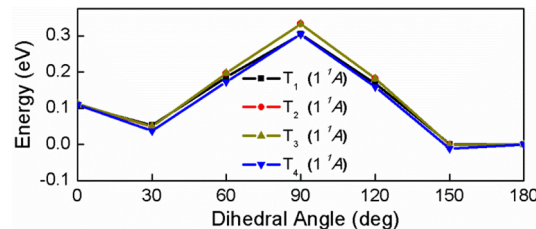


**Figure 3.** Ground state torsional potential energy curves for  $(PV)_7P$  for the four angles  $T_1$ ,  $T_2$ ,  $T_3$ , and  $T_4$ . The ground state energy minimum is taken as reference.

similar. For  $T_1$ ,  $T_2$ , and  $T_3$  the planar geometry displayed in Scheme 3 (torsional angle  $180^\circ$ ) is the most stable one, showing a very flat potential surface until  $150^\circ$ . For  $T_4$ , the geometry with a torsional angle of  $150^\circ$  is most stable by a small margin of 0.011 eV. In all cases the maximum lies at  $90^\circ$  with a barrier of 0.30 eV for  $T_1$  and the other barrier heights within 0.03 eV.

Torsional potential curves computed for the first four excited states are shown in Figure 4 for the angles  $T_1$ – $T_4$ . For all torsions and for all four excited states the planar geometry with a dihedral angle of  $180^\circ$  is the most stable one. The barrier to the torsional rotation is located at an angle of  $90^\circ$  in all cases. At the planar geometries the four excited states investigated are well separated. But as the torsional angle changes, for  $T_1$  and  $T_2$  the energies of the  $S_1$  and  $S_2$  states and  $S_3$  and  $S_4$  states approach each other. At  $90^\circ$  they are pairwise almost degenerate. For  $T_3$ , the  $S_2$  and  $S_3$  states become almost degenerate at  $90^\circ$  and for  $T_4$  the same situation happens for the  $S_3$  and  $S_4$  states while at the same time the other two states remain separate from each other. A rationalization of this situation will be given on the basis of the characteristics of the orbitals investigated in the following paragraph and the discussion in section 3.4.

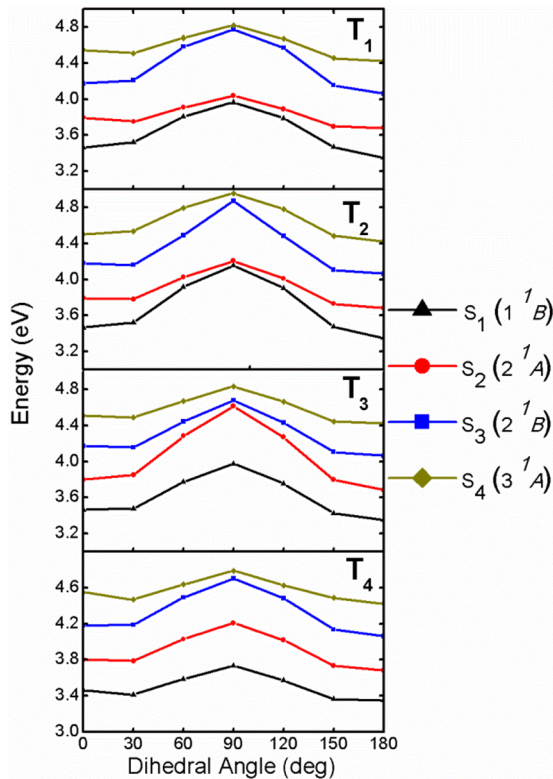


**Figure 4.** Excited state torsional potential energy curves for  $(PV)_7P$  for the four angles  $T_1$ ,  $T_2$ ,  $T_3$ , and  $T_4$ . The planar ground state energy minimum is taken as reference.

The two highest occupied and the two lowest unoccupied orbitals of the planar  $(PV)_7P$  oligomer are depicted in Figure 5.

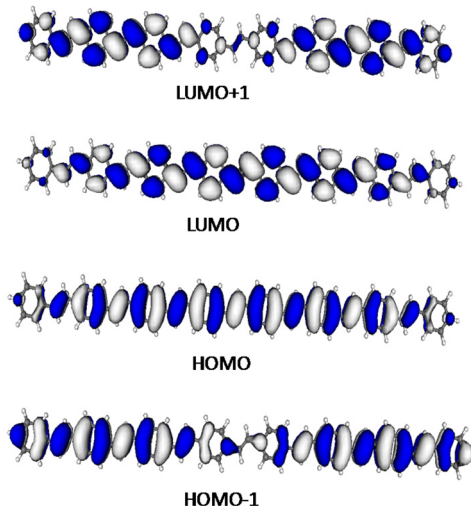


**Figure 5.** Orbital plots for  $(PV)_7P$  in planar geometry.

Inspection of this figure shows that the highest occupied molecular orbital (HOMO) and the lowest unoccupied molecular orbital (LUMO) have their maximal amplitudes in the middle of the chain whereas the HOMO-1 and LUMO+1 orbitals have two regions of maximal amplitudes in each of the halves of the chain. From Table 1S of the Supporting Information it is observed that for the planar geometry the lowest electronic excitation is dominated by a HOMO  $\rightarrow$  LUMO transition followed by a smaller contribution from

HOMO-1 to LUMO1. On twisting the planar geometry around any of the torsional angles, the participation of the HOMO-1 to LUMO+1 transition increases and the contribution of the HOMO  $\rightarrow$  LUMO transition simultaneously decreases. Finally, for 90°, the contributions from HOMO-LUMO and HOMO-1  $\rightarrow$  LUMO+1 transitions are almost the same for all of the four torsional angles. Thereafter, the importance of the HOMO  $\rightarrow$  LUMO transition slowly increases again. Plots of the frontier orbitals for  $T_1$  (Figure 6)

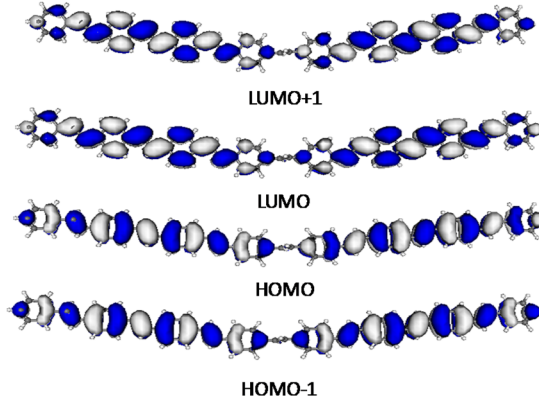


**Figure 6.** Orbital plots for  $(PV)_7P$  at 90°  $T_1$  torsion.

and  $T_2$  (Figure 3S, Supporting Information) at 90° show for the four orbitals HOMO-1 to LUMO+1 two regions separated by an extended nodal area in the center. For  $T_3$  (Figure 4S, Supporting Information), the HOMO and LUMO are again concentrated in the center whereas the (HOMO-1 and LUMO+1) pair is concentrated at the chain ends. In case of  $T_4$  (Figure 5S, Supporting Information), the HOMO and LUMO are again localized in the middle of the chain and there is negligible participation of the phenyl rings at the ends of the chain.

To examine the effect of the addition of an extra terminal vinyl group, rigid  $T_1$  potential energy curves have been calculated for  $(PV)_8$ . The resulting curves (Figure 7) are very similar to the ones obtained for torsion  $T_1$  in  $(PV)_7P$  (Figure 4). Again, the first excited state has its global minimum at a planar geometry and the states  $S_1$  and  $S_2$  approach each other along the torsion and become closest at 90°. Thus, removing

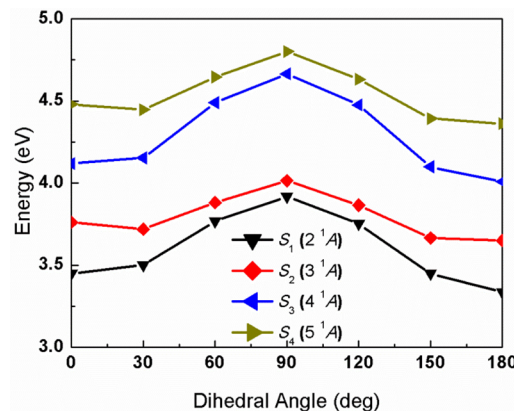


**Figure 7.** Potential energy curves for the central torsion for the first four excited states of  $(PV)_8$ . The ground state energy minimum at  $\tau = 180^\circ$  is taken as reference.

the equivalence of the two chain halves in  $(PV)_7P$  due to the  $C_2$  symmetry by introducing the terminal vinyl group has only a minor influence on the torsional potentials.

The effect of geometry relaxation has been tested for the  $T_1$  rotation in  $S_0$  and  $S_1$ . These curves were computed by fixing the torsional angle  $T_1$  and optimizing the remaining geometry parameters using a  $C_2$  symmetry restraint. Results are displayed in Figure 8. For the ground state, the geometry with a dihedral

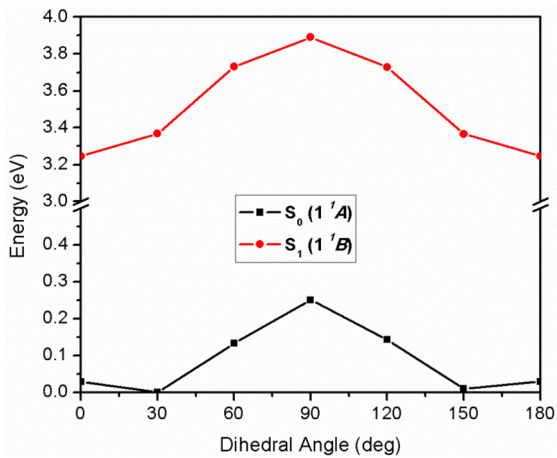


**Figure 8.** Relaxed potential energy curves for the ground state and the first excited states of  $(PV)_7P$  for the torsional angle  $T_1$ . The ground state energy minimum at  $\tau = 30^\circ$  is taken as reference.

angle of  $30^\circ$  is the most stable configuration. The stabilization with respect to the planar structure is, however, quite small and amounts to 0.03 eV. The barrier height with respect to the  $90^\circ$  barrier is 0.25 eV. For comparison, the barrier computed from the rigid rotation is 0.30 eV. The structure with the dihedral angle of  $150^\circ$  is only 0.01 eV higher in energy than the most stable structure at  $30^\circ$ . For the first excited state, the planar geometries are the most stable ones and the overall shape of the torsional curve is similar to the one of the rigid  $T_1$  rotation (Figure 4). The entire relaxed  $S_1$  torsional curve is stabilized due to the geometry optimization in comparison to the one computed for the rigid rotation. This stabilization amounts to 0.105 eV for the planar structure at  $180^\circ$  and to 0.07 eV at  $90^\circ$ . As a result, the rotational  $T_1$  barrier is increased by about 0.035–0.335 eV.

**3.4. Character of the Excited States.** To get a more detailed insight into the excited states, an analysis of the charge transfer numbers (eq 3) was carried out. The results are presented in Figure 9. In each of these diagrams the position of the *hole* and *electron* are plotted along the vertical and horizontal axes, respectively, with eight boxes in each direction representing the eight PV units. In these boxes the value of  $\Omega_{AB}^\alpha$ , which amounts to the probability of simultaneously finding the *hole* on fragment A and the *electron* on fragment B, is coded in grayscale. The length of the exciton is seen along the diagonal of the plot, whereas the *electron hole* separation (charge transfer character) is represented by the off-diagonal width. At the planar equilibrium geometry the three lowest excited states can be seen as rather tightly bound excitons with small off-diagonal width. The  $\Omega_{AB}^\alpha$  plot for  $S_2$  differs from that for  $S_1$  by a region of low amplitude in the center. This difference originates from a nodal plane in the excitonic wave function. Similarly, the  $\Omega_{AB}^\alpha$  plot for  $S_3$  indicates two nodal planes. An interpretation of this nodal progression has been

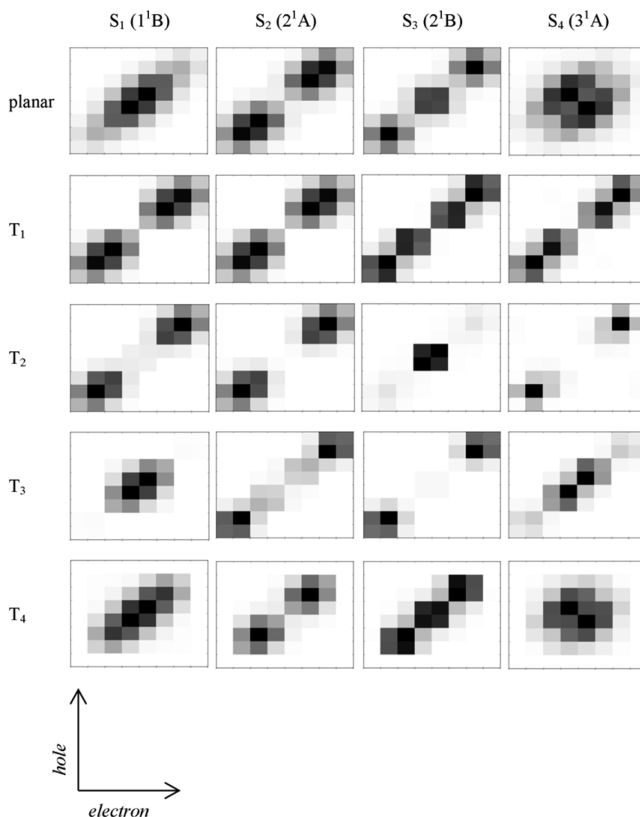


**Figure 9.** Plots of the charge transfer numbers  $\Omega_{AB}^\alpha$  (eq 6) for the first four singlet excited states of  $(PV)_7P$  at its planar geometry and after  $90^\circ$  torsion around the  $T_1$ ,  $T_2$ ,  $T_3$ , and  $T_4$  angle, respectively. The axis of each square numbers the eight phenylenevinylene units (going from left to right and bottom to top, respectively). The value of  $\Omega_{AB}^\alpha$  is coded in grayscale tone.

given by Wu et al.<sup>51</sup> in terms of a particle-in-a-box model. Thus, these three states can be seen as belonging to the same exciton band that would arise at infinite chain length. This fact is also consistent with the observation made above that the excitation energies of these three states converge to the same value at infinite chain length (Figure 1). The torsion around  $T_1$  at an angle of  $90^\circ$  creates a break in the middle of the chain (see the MOs in Figure 6) dividing the molecule into two equivalent weakly coupled fragments.  $S_1/S_2$  and  $S_3/S_4$  form two pairs of states of very similar excited state structures. These pairs could each be seen as the positive and negative linear combinations of two localized fragment states. The small gap between each of these pairs of states (Figure 4,  $T_1$ ) can be directly identified with the splitting due to excitonic coupling. For the next two torsions ( $T_2$ ,  $T_3$ ) at  $90^\circ$ , the oligomer is effectively split into three parts, two border units and the center unit. For the  $90^\circ$  structure around  $T_2$ ,  $S_1$  and  $S_2$  can be identified as a pair of excitons on the outer fragments, showing a respective small energy splitting in Figure 4. The  $\Omega_{AB}^\alpha$  plots for  $S_3$  and  $S_4$  exhibit a completely different excited state structure. This suggests that their near-degeneracy in Figure 4 is only accidental. For the case of  $T_3$  the near-degenerate  $S_2$  and  $S_3$  states can be approximately identified as a pair of excitons. In the case of  $T_4$ , only the two outer PV units are twisted and thereby decoupled. This leads to a central conjugated planar region of the remaining chain. Therefore, the first four excited states have similar appearances to the planar equilibrium structure. The  $T_4$  structure at  $90^\circ$  can be seen as  $(PV)_5P$  with two additional

decoupled end groups and the low splitting between  $S_3$  and  $S_4$  can be understood to derive just from the same type of accidental degeneracy that was present for these two states in planar  $(\text{PV})_5\text{P}$  (Figure 1).

#### 4. CONCLUSION

The lowest four  $\pi-\pi^*$  transitions in the series of PPV oligomers have been investigated by means of the ab initio RI-ADC(2) method. It has been shown that this method is well suited to describe vertical excitations within the  $\pi$  system of PPV and that also excited state geometry optimizations can be performed reliably. In contrast to the TDDFT approach,<sup>14</sup> ADC(2) does not suffer from an intrinsic bias toward defect localization or delocalization in the excited state of PPV. Moreover, due to the resolution of the identity approach, efficient calculations of sufficiently large oligomers sizes could be performed, which are of direct use for describing polymer properties for the excited state. Two important types of structural parameters characterizing the excited state relaxation of PPV have been investigated in detail. The BLA displays the characteristic quinoid distortions found by means of geometry relaxation in the lowest excited singlet state of conjugated polymers, which could be quantified at high computational level by our calculations.<sup>8,10,24</sup> The torsional modes give insight into the excitonic coupling for several excited states, which has, to our knowledge, not been investigated in detail so far. Combined with the analysis of transition density matrices, an overall picture of the relation of these excited states has been given that should provide a useful benchmark for calculations using lower level, but computationally more efficient, methods.

The present results show the most likely local relaxation pathway after Franck–Condon excitation, the self-trapping<sup>8</sup> of the exciton in the  $S_1$  state by BLA relaxation as shown in Figure 3. However, vibrational energy relaxation is not immediate, and coherent BLA oscillations may be observed on a time scale of tens to hundreds of femtoseconds.<sup>52</sup> The EET dynamics, which will compete with the trapping process, can be anticipated from the splitting of the exciton on torsions along the vinylene C–C bonds (Figure 9) and the concomitant excitonic couplings. A strong coupling between electron and phonon motions can be expected both for the trapping and for the EET process. The analysis of transition densities indicates for the planar  $(\text{PV})_7\text{P}$  molecule the emergence of an excitonic band structure. A significant change in the excited states followed from torsions around the vinylene junctions. Consequently, the qualitative picture of the excitonic interactions depends significantly on the location of the torsion within the oligomer. In the extreme case of a 90° torsion around the central vinylene bond, electronic decoupling and the formation of pairs of equivalent excitonic states could be observed. For torsions around the other vinylene C–C bonds a more complex pattern deriving from the presence of three decoupled fragments was found. In a subsequent work,<sup>39</sup> the present electronic structure results will be employed to parametrize an effective Frenkel exciton Hamiltonian.<sup>39</sup> This ab initio-based diabatic model Hamiltonian will be used as the basis for quantum dynamical simulations of ultrafast exciton transfer dynamics in PPV type systems.

#### ■ ASSOCIATED CONTENT

##### Supporting Information

Excited state energies ( $S_1$ – $S_4$ ) for different torsional angles around the torsions  $T_1$ – $T_4$  are collected in Tables 3S–4S. The

direction of transition dipole moments are shown in Figure 1S, computed bond lengths in Figure 2S, and MO plots for 90° torsions around  $T_2$ – $T_4$  are depicted in Figures 3S–5S. This material is available free of charge via the Internet at <http://pubs.acs.org>.

#### ■ AUTHOR INFORMATION

##### Corresponding Author

\*E-mail: H.L., [hans.lischka@univie.ac.at](mailto:hans.lischka@univie.ac.at); I.B., [burghardt@chemie.uni-frankfurt.de](mailto:burghardt@chemie.uni-frankfurt.de).

##### Notes

The authors declare no competing financial interest.

#### ■ ACKNOWLEDGMENTS

A.N.P. gratefully acknowledges a BOYSCAST fellowship allowing him a stay at Ecole Normale Supérieure, Paris, during the period July 2010 to June 2011. This work has been supported by the Austrian Science Fund within the framework of the Special Research Program F41, Vienna Computational Materials Laboratory (ViCoM). This material is based upon work supported by the National Science Foundation under CHE-1213263. Support was provided by the Robert A.Welch Foundation under Grant No. D-0005. F.P. is a recipient of a DOC fellowship of the Austrian Academy of Sciences. The calculations were performed at the Vienna Scientific Cluster (project nos. 70019 and 70151).

#### ■ REFERENCES

- (1) Meier, H.; Stalmach, U.; Kolshorn, H. Effective Conjugation Length and UV/VIS Spectra of Oligomers. *Acta Polym.* **1997**, *48*, 379–384.
- (2) Bredas, J. L.; Cornil, J.; Beljonne, D.; dos Santos, D.; Shuai, Z. G. Excited-State Electronic Structure of Conjugated Oligomers and Polymers: A Quantum-Chemical Approach to Optical Phenomena. *Acc. Chem. Res.* **1999**, *32*, 267–276.
- (3) Peeters, E.; Ramos, A. M.; Meskers, S. C. J.; Janssen, R. A. J. Singlet and Triplet Excitations of Chiral Dialkoxy-P-Phenylene Vinylene Oligomers. *J. Chem. Phys.* **2000**, *112*, 9445–9454.
- (4) Kirova, N. Understanding Excitons in Optically Active Polymers. *Polym. Int.* **2008**, *57*, 678–688.
- (5) Collini, E.; Scholes, G. D. Coherent Intrachain Energy Migration in a Conjugated Polymer at Room Temperature. *Science* **2009**, *323*, 369–373.
- (6) Bredas, J. L.; Silbey, R. Excitons Surf Along Conjugated Polymer Chains. *Science* **2009**, *323*, 348–349.
- (7) Bredas, J. L.; Norton, J. E.; Cornil, J.; Coropceanu, V. Molecular Understanding of Organic Solar Cells: The Challenges. *Acc. Chem. Res.* **2009**, *42*, 1691–1699.
- (8) Tretiak, S.; Saxena, A.; Martin, R. L.; Bishop, A. R. Conformational Dynamics of Photoexcited Conjugated Molecules. *Phys. Rev. Lett.* **2002**, *89* (097402), 1–4.
- (9) Fernandez-Alberti, S.; Kleiman, V. D.; Tretiak, S.; Roitberg, A. E. Unidirectional Energy Transfer in Conjugated Molecules: The Crucial Role of High-Frequency C C Bonds. *J. Phys. Chem. Lett.* **2010**, *1*, 2699–2704.
- (10) Sterpone, F.; Rossky, P. J. Molecular Modeling and Simulation of Conjugated Polymer Oligomers: Ground and Excited State Chain Dynamics of PPV in the Gas Phase. *J. Phys. Chem. B* **2008**, *112*, 4983–4993.
- (11) Karabunarliev, S.; Bittner, E. R. Polaron-Excitons and Electron-Vibrational Band Shapes in Conjugated Polymers. *J. Chem. Phys.* **2003**, *118*, 4291–4296.
- (12) Lukes, V.; Solc, R.; Barbatti, M.; Lischka, H.; Kauffmann, H. F. Torsional Potentials and Full-Dimensional Simulation of Electronic Absorption Spectra of Para-Phenylenevinylene Oligomers Using

- Semiempirical Hamiltonians. *J. Theor. Comput. Chem.* **2010**, *9*, 249–263.
- (13) Pogantsch, A.; Heimel, G.; Zojer, E. Quantitative Prediction of Optical Excitations in Conjugated Organic Oligomers: A Density Functional Theory Study. *J. Chem. Phys.* **2002**, *117*, 5921–5928.
- (14) Nayyar, I. H.; Batista, E. R.; Tretiak, S.; Saxena, A.; Smith, D. L.; Martin, R. L. Localization of Electronic Excitations in Conjugated Polymers Studied by Dft. *J. Phys. Chem. Lett.* **2011**, *2*, 566–571.
- (15) Nayyar, I. H.; Batista, E. R.; Tretiak, S.; Saxena, A.; Smith, D. L.; Martin, R. L. Role of Geometric Distortion and Polarization in Localizing Electronic Excitations in Conjugated Polymers. *J. Chem. Theory Comput.* **2013**, *9*, 1144–1154.
- (16) Sterpone, F.; Martinazzo, R.; Panda, A. N.; Burghardt, I. Coherent Excitation Transfer Driven by Torsional Dynamics: A Model Hamiltonian for PPV Type Systems. *Z. Phys. Chem.* **2011**, *225*, 541–551.
- (17) Beljonne, D.; Pourtois, G.; Silva, C.; Hennebicq, E.; Herz, L. M.; Friend, R. H.; Scholes, G. D.; Setayesh, S.; Mullen, K.; Bredas, J. L. Interchain Vs. Intrachain Energy Transfer in Acceptor-Capped Conjugated Polymers. *Proc. Natl. Acad. Sci. U. S. A.* **2002**, *99*, 10982–10987.
- (18) Singh, J.; Bittner, E. R.; Beljonne, D.; Scholes, G. D. Fluorescence Depolarization in Poly[2-Methoxy-5-((2-Ethylhexyl)-Oxy)-1,4-Phenylenevinylene]: Sites Versus Eigenstates Hopping. *J. Chem. Phys.* **2009**, *131* (194905), 1–10.
- (19) Molina, V.; Merchan, M.; Roos, B. O. Theoretical Study of the Electronic Spectrum of Trans-Stilbene. *J. Phys. Chem. A* **1997**, *101*, 3478–3487.
- (20) Saha, B.; Ehara, M.; Nakatsuji, H. Investigation of the Electronic Spectra and Excited-State Geometries of Poly(Para-Phenylene Vinylene) (PPV) and Poly(Para-Phenylene) (PP) by the Symmetry-Adapted Cluster Configuration Interaction (SAC-CI) Method. *J. Phys. Chem. A* **2007**, *111*, 5473–5481.
- (21) Quenneville, J.; Martinez, T. J. Ab Initio Study of Cis-Trans Photoisomerization in Stilbene and Ethylene. *J. Phys. Chem. A* **2003**, *107*, 829–837.
- (22) Christiansen, O.; Koch, H.; Jorgensen, P. The 2nd-Order Approximate Coupled-Cluster Singles and Doubles Model CC2. *Chem. Phys. Lett.* **1995**, *243*, 409–418.
- (23) V, L.; Aquino, A. J. A.; Lischka, H. Theoretical Study of Vibrational and Optical Spectra of Methylenes-Bridged Oligofluorenes. *J. Phys. Chem. A* **2005**, *109*, 10232–10238.
- (24) Lukes, V.; Aquino, A. J. A.; Lischka, H.; Kauffmann, H. F. Dependence of Optical Properties of Oligo-Para-Phenylens on Torsional Modes and Chain Length. *J. Phys. Chem. B* **2007**, *111*, 7954–7962.
- (25) Hattig, C. Geometry Optimizations with the Coupled-Cluster Model CC2 Using the Resolution-of-the-Identity Approximation. *J. Chem. Phys.* **2003**, *118*, 7751–7761.
- (26) Kohn, A.; Hattig, C. Analytic Gradients for Excited States in the Coupled-Cluster Model CC2 Employing the Resolution-of-the-Identity Approximation. *J. Chem. Phys.* **2003**, *119*, 5021–5036.
- (27) Schreiber, M.; Silva, M. R.; Sauer, S. P. A.; Thiel, W. Benchmarks for Electronically Excited States: CASPT2, CC2, CCSD, and CC3. *J. Chem. Phys.* **2008**, *128* (134110), 1–25.
- (28) Trofimov, A. B.; Schirmer, J. An Efficient Polarization Propagator Approach to Valence Electron-Excitation Spectra. *J. Phys. B-At. Mol. Opt.* **1995**, *28*, 2299–2324.
- (29) Hattig, C. Structure Optimizations for Excited States with Correlated Second-Order Methods: CC2 and ADC(2). *Adv. Quantum Chem.* **2005**, *50*, 37–60.
- (30) Aquino, A. J. A.; Nachtigalova, D.; Hobza, P.; Truhlar, D. G.; Hattig, C.; Lischka, H. The Charge-Transfer States in a Stacked Nucleobase Dimer Complex: A Benchmark Study. *J. Comput. Chem.* **2011**, *32*, 1217–1227.
- (31) Szalay, P. G.; Watson, T.; Perera, A.; Lotrich, V. F.; Bartlett, R. J. Benchmark Studies on the Building Blocks of DNA. 1. Superiority of Coupled Cluster Methods in Describing the Excited States of Nucleobases in the Franck-Condon Region. *J. Phys. Chem. A* **2012**, *116*, 6702–6710.
- (32) Plasser, F.; Lischka, H. Analysis of Excitonic and Charge Transfer Interactions from Quantum Chemical Calculations. *J. Chem. Theory Comput.* **2012**, *8*, 2777–2789.
- (33) Heimel, G.; Pogantsch, A.; Zojer, E. Exciton-Phonon Coupling in Conjugated Organic Molecules. *Phys. Scr.* **2004**, *T109*, 156–158.
- (34) Tozer, O. R.; Barford, W. Exciton Dynamics in Disordered Poly(P-Phenylenevinylene). 1. Ultrafast Interconversion and Dynamical Localization. *J. Phys. Chem. A* **2012**, *116*, 10310–10318.
- (35) Barford, W.; Lidzey, D. G.; Makhov, D. V.; Meijer, A. J. H. Exciton Localization in Disordered Poly(3-Hexylthiophene). *J. Chem. Phys.* **2010**, *133* (044504), 1–6.
- (36) Beenken, W. J. D.; Pullerits, T. Spectroscopic Units in Conjugated Polymers: A Quantum Chemically Founded Concept? *J. Phys. Chem. B* **2004**, *108*, 6164–6169.
- (37) Beenken, W. J. D. Excitons in Conjugated Polymers: Do We Need a Paradigm Change? *Phys Status Solidi A* **2009**, *206*, 2750–2756.
- (38) Westenhoff, S.; Beenken, W. J. D.; Friend, R. H.; Greenham, N. C.; Yartsev, A.; Sundstrom, V. Anomalous Energy Transfer Dynamics Due to Torsional Relaxation in a Conjugated Polymer. *Phys. Rev. Lett.* **2006**, *97* (166804), 1–4.
- (39) Binder, R.; Römer, S.; Plasser, F.; Panda, A. N.; Aquino, A. J. A.; Lischka, H.; Burghardt, I. Unpublished work.
- (40) Moller, C.; Plesset, M. S. Note on an Approximation Treatment for Many-Electron Systems. *Phys. Rev.* **1934**, *46*, 0618–0622.
- (41) Weigend, F.; Haser, M.; Patzelt, H.; Ahlrichs, R. RI-MP2: Optimized Auxiliary Basis Sets and Demonstration of Efficiency. *Chem. Phys. Lett.* **1998**, *294*, 143–152.
- (42) Hattig, C.; Weigend, F. CC2 Excitation Energy Calculations on Large Molecules Using the Resolution of the Identity Approximation. *J. Chem. Phys.* **2000**, *113*, 5154–5161.
- (43) Hattig, C.; Kohn, A. Transition Moments and Excited-State First-Order Properties in the Coupled-Cluster Model CC2 Using the Resolution-of-the-Identity Approximation. *J. Chem. Phys.* **2002**, *117*, 6939–6951.
- (44) Schafer, A.; Horn, H.; Ahlrichs, R. Fully Optimized Contracted Gaussian-Basis Sets for Atoms Li to Kr. *J. Chem. Phys.* **1992**, *97*, 2571–2577.
- (45) Schafer, A.; Huber, C.; Ahlrichs, R. Fully Optimized Contracted Gaussian-Basis Sets of Triple Zeta Valence Quality for Atoms Li to Kr. *J. Chem. Phys.* **1994**, *100*, 5829–5835.
- (46) Kuhn, W. Über Das Absorptionspektrum Der Polyene. *Helv. Chim. Acta* **1948**, *31*, 1780–1799.
- (47) Gierschner, J.; Cornil, J.; Egelhaaf, H. J. Optical Bandgaps of Pi-Conjugated Organic Materials at the Polymer Limit: Experiment and Theory. *Adv. Mater.* **2007**, *19*, 173–191.
- (48) Tretiak, S.; Mukamel, S. Density Matrix Analysis and Simulation of Electronic Excitations in Conjugated and Aggregated Molecules. *Chem. Rev.* **2002**, *102*, 3171–3212.
- (49) Luzanov, A. V.; Zhikol, O. A. Electron Invariants and Excited State Structural Analysis for Electronic Transitions within CIS, RPA, and TDDFT Models. *Int. J. Quantum Chem.* **2010**, *110*, 902–924.
- (50) Gierschner, J.; Mack, H. G.; Luer, L.; Oelkrug, D. Fluorescence and Absorption Spectra of Oligophenylenevinylenes: Vibronic Coupling, Band Shapes, and Solvatochromism. *J. Chem. Phys.* **2002**, *116*, 8596–8609.
- (51) Wu, C.; Malinin, S. V.; Tretiak, S.; Chernyak, V. Y. Exciton Scattering Approach for Branched Conjugated Molecules and Complexes. III. Applications. *J. Chem. Phys.* **2008**, *129* (174113), 1–7.
- (52) Lanzani, G.; Cerullo, G.; Brabec, C.; Sariciftci, N. S. Time Domain Investigation of the Intrachain Vibrational Dynamics of a Prototypical Light-Emitting Conjugated Polymer. *Phys. Rev. Lett.* **2003**, *90* (047402), 1–4.